Check for updates

Journal of Medical Virology

WILEY

JOURNAL OF MEDICAL VIROLOGY

SHORT COMMUNICATION OPEN ACCESS

The Open Reading Frame 7b of the SARS-CoV-2 Disperse Trans-Golgi and Activate the NLRP3 Inflammasome

Julio García-Villalba[1] | Laura Hurtado-Navarro[1] | Diego Angosto-Bazarra[1] | Alberto Baroja-Mazo[1] | Pablo Pelegrin[1,2]

[1]Biomedical Research Institute of Murcia (IMIB), University Clinical Hospital Virgen Arrixaca, Murcia, Spain | [2]Department of Biochemistry and Molecular Biology B and Immunology, Faculty of Medicine, University of Murcia, Murcia, Spain

Correspondence: Pablo Pelegrin (pablopel@um.es)

Received: 19 May 2025 | **Revised:** 6 February 2026 | **Accepted:** 13 March 2026

Funding: Instituto de Salud Carlos III; Fundación Séneca; Ministerio de Ciencia e Innovación

Keywords: ASC speck | COVID-19 | IL-1 | inflammation | NLRP3 | SARS-CoV-2

ABSTRACT

Inflammasomes orchestrate the inflammatory response against bacterial and viral infections, thereby initiating the synthesis of pro-inflammatory cytokines, mainly IL-1β and IL-18. SARS-CoV-2 infection induces an inflammatory response mediated by the activation of NLRP1 and NLRP3 inflammasomes. In this study, we demonstrated that the open reading frame 7b (ORF7b) accessory protein of SARS-CoV-2 induces the NLRP3 inflammasome in a recombinant HEK293T model. This resulted in an increase in the distribution of NLRP3 puncta, ASC-specking cells, and caspase-1 activation. ORF7b expression also induced the dispersion of the trans-Golgi network, a well-known step in the activation of the NLRP3 inflammasome. This study proposes a novel additional mechanism by which SARS-CoV-2 promotes NLRP3 inflammasome activation by ORF7b.

1 | Introduction

Inflammasomes are intracellular multiprotein complexes assembled in response to pathogen- and danger-associated molecular patterns (PAMPs and DAMPs respectively). These complexes trigger the activation of caspase-1 and induce the release of the inflammatory cytokines interleukin (IL)-1β and IL-18 via gasdermin D (GSDMD) induced pyroptosis [1–3]. SARS-CoV-2 infection triggers the activation of different inflammasomes, including the ones formed by the nucleotide-binding oligomerization domain, leucine rich repeat and pyrin domain containing-protein 1 (NLRP1), NLRP3, caspase recruitment domain-containing protein 8 (CARD8) and absent in melanoma 2 (AIM2) (Supporting Table 1) [4–22]. Both IL-1β and IL-18 cytokines have been associated with COVID-19 and the severity of the acute respiratory distress syndrome [23–28]. Clinical trials involving recombinant IL-1 receptor antagonist anakinra demonstrated a reduction in the severity of respiratory failure and the inflammatory response [29].

The inflammasome formed by the NLRP3 is mainly triggered by different PAMPs and DAMPs that disturb intracellular K^+ concentration, which in turn disperses trans-Golgi network (TGN), affecting mitochondria ATP production and reactive oxygen production (ROS) [30–33]. Different compounds block the NLRP3 inflammasome [34, 35], and blockade using the specific inhibitor MCC950 effectively diminished lung inflammation in human ACE2 transgenic mice infected with live SARS-CoV-2 [36]. SARS-CoV-2 can activate the NLRP3 inflammasome by several distinct mechanisms [4–22]. In particular the expression of ORF3a triggers cellular K^+ efflux to activate NLRP3 [13–15], the expression of the N protein and the ORF8 encoded protein are able to interact with NLRP3 and induce its activation [5, 37], and ORF9b homodimers cause mitochondrial eviction and NLRP3 activation [18]. During SARS-CoV-2 infection there is a reprogramming of the host macrophages, making them able to be primed for the NLRP3 inflammasome by the virus spike (S) protein [9]. As a compensatory mechanism, SARS-CoV-2 virus infection also results

This is an open access article under the terms of the Creative Commons Attribution-NonCommercial License, which permits use, distribution and reproduction in any medium, provided the original work is properly cited and is not used for commercial purposes.

© 2026 The Author(s). *Journal of Medical Virology* published by Wiley Periodicals LLC.

in a blockage of the inflammasome at different levels, for example, the envelope (E) protein impairs NLRP3 priming [12], the non-structural proteins 1 and 13 suppress the activation of the NLRP3 inflammasome [38] and the N protein cleaves GSDMD within the N-terminal lytic domain inactivating pyroptosis [39]. Therefore, there is a fine balance of the NLRP3 inflammasome activity during SARS-CoV-2 infection.

In this study, we have found that the ORF7b accessory protein of SARS-CoV-2 favours the activation of NLRP3, increasing ASC speck formation and caspase-1 activation. ORF7b promoted dispersion of the trans-Golgi network and activation of NLRP3. ORF7b gene is conserved across the different variants of SARS-CoV-2 and other coronaviruses, suggesting that the ability of ORF7b to disperse trans-Golgi network could be a shared feature of coronaviruses.

2 | Results

To investigate the potential effect of SARS-CoV-2 in the activation of NLRP3, we used a well-established recombinant system using HEK293T cells expressing human wild-type NLRP3 YFP tagged. Treatment of these cells with NLRP3 activators have previously shown to change the distribution of NLRP3 fluorescence from homogeneous in the cytosol to a puncta distribution [30, 32]. We initially expressed the different SARS-CoV-2 proteins in these cells by transient transfections, and found that from the 25 different SARS-CoV-2 protein tested, the expression of ORF10, Nsp4, Nsp6, Nsp8, Nsp11, and Nsp14 was not detectable by Western blot (Supporting Figure 1). We then quantify the percentage of transfected cells with a puncta distribution of NLRP3 and found that it increased upon expression of the structural protein E and the ORF7b (Figure 1A, Supporting Figure 2). After repeating the experiments expressing the protein

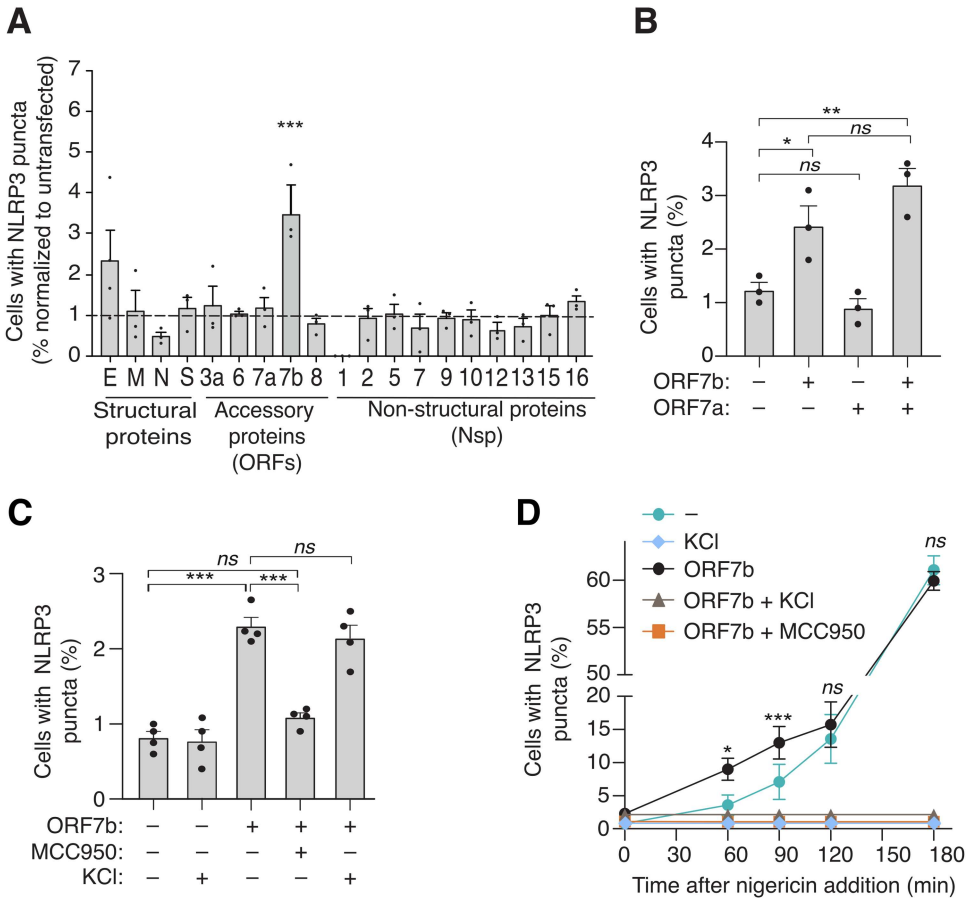

FIGURE 1 | The ORF7b from SARS-CoV-2 increase puncta distribution of NLRP3. (A) Percentage of HEK293T cells with a NLRP3-YFP puncta distribution after 48 h of transfection with different plasmids encoding for SARS-CoV-2 proteins. Dotted line represents the basal number of cells with NLRP3 puncta found in control transfections with an empty pcDNA vector, value used to normalize the number of cells with NLRP3 puncta for the different transfections. (B, C) HEK293T cells with a NLRP3-YFP puncta distribution after 48 h of transfection with empty pcDNA vector (–) or plasmids encoding for SARS-CoV-2 ORF7a and/or ORF7b proteins (B, C) in the presence or absence of 10 μM of MCC950 or a buffer containing 40 μM of KCl (C). Percentage of transfected cells with a NLRP3 puncta distribution is represented. (D) HEK293T cells with a NLRP3-YFP puncta distribution after 48 h of transfection with empty pcDNA vector (–) or a plasmid encoding for SARS-CoV-2 ORF7b protein and then treated for 60, 90, 120, or 180 min with nigericin (10 μM) in the presence or absence of 10 μM of MCC950 or a buffer containing 40 μM of KCl. Percentage of transfected cells with a NLRP3 puncta distribution is represented. For A–C each dot represents an independent experiment, and data are represented as mean (grey bars) ± s.e.m; For D, each dot represents de mean of 4 independent experiments. Each independent experiment was performed in duplicate biological replicates and for each 9 (A–C) or 5 (D) different random fields of view were quantified with an approximate total number of counted cells of 1350 for A–C or 320 for D in each independent experiment. One-way ANOVA with Holm-Sidak's multiple-comparisons test was used for A–D; ****$p < 0.0001$, ***$p > 0.0001 < 0.001$, **$p > 0.001 < 0.01$, *$p > 0.01 < 0.05$, $p > 0.05$ not significant (*ns*).

10969071, 2026, 4, Downloaded from https://onlinelibrary.wiley.com/doi/10.1002/jmv.70894 by Servicio Murciano De Salud, Wiley Online Library on [31/03/2026]. See the Terms and Conditions (https://onlinelibrary.wiley.com/terms-and-conditions) on Wiley Online Library for rules of use; OA articles are governed by the applicable Creative Commons License

E or the ORF7b we found a significant increase induced by both the protein E and ORF7b (Supporting Figure 3 A). While SARS-CoV-2 protein E has been previously demonstrated to activate NLRP3 [12, 13] (Supporting Table 1), the role of ORF7b in inducing the NLRP3 inflammasome remains largely unexplored. ORF7b is an accessory protein found in different coronavirus, and its sequence was found conserved among the different SARS-CoV-2 variants (Supporting Figure 3B), suggesting that the ORF7b of these coronavirus variants could exert the same effect on NLRP3 activation. However, SARS-CoV-2 ORF7b acquired the F19L mutation within the JN.1 linage of the Omicron variant (Supporting Figure 3B). While phenylalanine and leucine are both hydrophobic amino acids, and this mutation would not directly affect the overall structure of ORF7b, the functional implications of this variant warrant further evaluation. Although ORF7b derives from a shared transcript with ORF7a, they are differently translated proteins [40], therefore the overall sequence similarity among them is only of 9.4% in SARS-CoV-2. However, we observed that co-expression of ORF7a with ORF7b was not further increasing cells with NLRP3 puncta distribution (Figure 1B), but the NLRP3 inhibitor MCC950 was able to reduce the percentage of cells with puncta NLRP3 distribution induced by ORF7b (Figure 1C). However, blocking K^+ efflux from the cells using a high extracellular K^+ buffer did not affect ORF7b induced NLRP3 puncta distribution (Figure 1C). After cell stimulation with the K^+-ionophore nigericin, a well- established activator of NLRP3, we observed a marked elevation in the percentage of cells exhibiting NLRP3 puncta at relatively short time interval when the cells were expressing ORF7b (Figure 1D). This increase was a consequence of NLRP3 activation, as MCC950 decreased it, and dependent of intracellular K^+ efflux, as a buffer with KCl also decreased it (Figure 1D). As expected, the KCl buffer was also able to decrease nigericin-induced NLRP3 puncta distribution in cells do not expressing ORF7b (Figure 1D). Interestingly, from 2 to 3 h of nigericin stimulation, the presence of ORF7b was not able to increase the percentage of cells with puncta distribution of NLRP3 (Figure 1D), suggesting that ORF7b facilitate canonical NLRP3 activation at short times upon stimulation.

We next examined if the expression of ORF7b resulted in inflammasome formation by assessing caspase-1 activation. For that we expressed ASC and pro-caspase-1 in NLRP3 expressing cells with or without ORF7b expression. We observed increase of caspase-1 processing (p10 fragment) when ORF7b was expressed (Figure 2A). Similarly, when analysing the percentage of cells producing ASC oligomerisation by flow cytometry, we found that ORF7b, but not ORF7a, was able to increase of the percentage of cells with ASC oligomers (Figure 2B, Supporting Figure 4). The increase in caspase-1 activation and ASC oligomerisation was modest when nigericin was added to the cells (Figure 2C,D, Supporting Figure 4), but since ASC oligomerization is a fast process from the initial NLRP3 active structures, it has less resolution than the readout of NLRP3 puncta distribution when expressed without ASC as occurred in Figure 1D.

Additionally, human primary small airway epithelial cells (HSAEC) were used to investigate the role of ORF7b on NLRP3 activation. We found that these cells were expressing ASC (*PYCARD* gene), *CASP1* and *IL1B*, but not *NLRP3* (Figure 3A) and had to transfect a plasmid to express human NLRP3 in these cells. The basal expression of the inflammasome components *ASC* and *CASP1*, as well as *IL1B* and the transfection of NLRP3, bypass the classical requirement for a step 1 or priming of the NLRP3 inflammasome prior activation with the canonical activator nigericin. The expression of either ORF7a or ORF7b, was not affecting NLRP3 transfection and expression (Figure 3B). However, ORF7b expression upregulate *PYCARD*, *CASP1* and *IL1B* transcripts in HSAEC cells (Figure 3B). The co-expression of NLRP3 and ORF7b were not inducing IL-1β release (Figure 3C), but ORF7b increased the release of IL-1β after nigericin stimulation (Figure 3C).

Finally, since ORF7b from different coronavirus is expressed in the Golgi network [41, 42], we aimed to analyse if SARS-CoV-2 ORF7b affected *trans*-Golgi network (TGN). Expression of ORF7b, but not ORF7a, induced a dispersion of the TGN similarly to nigericin stimulation (Figure 4A). Of note, not all NLRP3 puncta co-localized with TGN dispersed structures under nigericin treatment or ORF7b expression (Figure 4A). This potentially suggests that not all NLRP3 puncta could represent active NLRP3 oligomers, and that a diversity of organelles or intracellular localizations could accumulate NLRP3 upon triggering stimulation. The dispersion of the TGN induced by ORF7b expression was independent on the NLRP3, as in HEK293T cells not expressing NLRP3, ORF7b was able to disperse TGN (Figure 4B). Overall, our data demonstrate that the ORF7b from SARS-CoV-2 localizes to the TGN of the cell and induces its dispersion, and that ORF7b expression is sufficient to facilitate NLRP3 inflammasome activation.

3 | Discussion

The immune response against SARS-CoV-2 has a strong inflammatory component, and in COVID-19 severe cases are related to an exacerbated inflammatory response [26, 28]. In fact, SARS-CoV-2 infection can activate multiple inflammasomes (Supporting Table 1) [4–22]. In the present study, we corroborate that the ORF7b accessory protein of SARS-CoV-2 could facilitate the activation of the NLRP3 inflammasome probably at relatively short time intervals via dispersion of the TGN. Different mechanism of SARS-CoV-2 have been proposed to activate the NLRP3 inflammasome, these include direct interaction with NLRP3, K^+ efflux via viroporins, mitochondria damage and ROS production, as well as transcriptional priming [9, 12–15]. On the other hand, the 3CL protease of SARS-CoV-2 is also able to cleave and activate the NLRP1 and CARD8 inflammasome by inducing N-terminal degradation [4, 22]. Our results suggest another mechanistic layer by which SARS-CoV-2 could facilitate NLRP3 inflammasome activation: TGN dispersion by ORF7b. ORF7b has been also identified in different coronavirus and has been localized to the Golgi [41, 42]. TGN dispersion has been found as a critical step needed for the activation of the NLRP3 inflammasome in response to K^+-efflux dependent and independent (imiquimod) activators [30], including influenza viral infection [43]. Here we found that the ORF7b of SARS-CoV-2 can disperse the TGN and facilitate NLRP3 activation, constituting a mechanism to affect the integrity of the TGN. However, our study shows that in the HEK293T recombinant system, the dispersion of the TGN induced by nigericin and/or ORF7b expression do not co-localize with the puncta distribution of NLRP3. Some puncta of NLRP3 are near TGN structures, but there are many TGN structures without NLRP3 and large NLRP3 puncta not localizing with TGN. This

10969071, 2026, 4, Downloaded from https://onlinelibrary.wiley.com/doi/10.1002/jmv.70894 by Servicio Murciano De Salud, Wiley Online Library on [31/03/2026]. See the Terms and Conditions (https://onlinelibrary.wiley.com/terms-and-conditions) on Wiley Online Library for rules of use; OA articles are governed by the applicable Creative Commons License

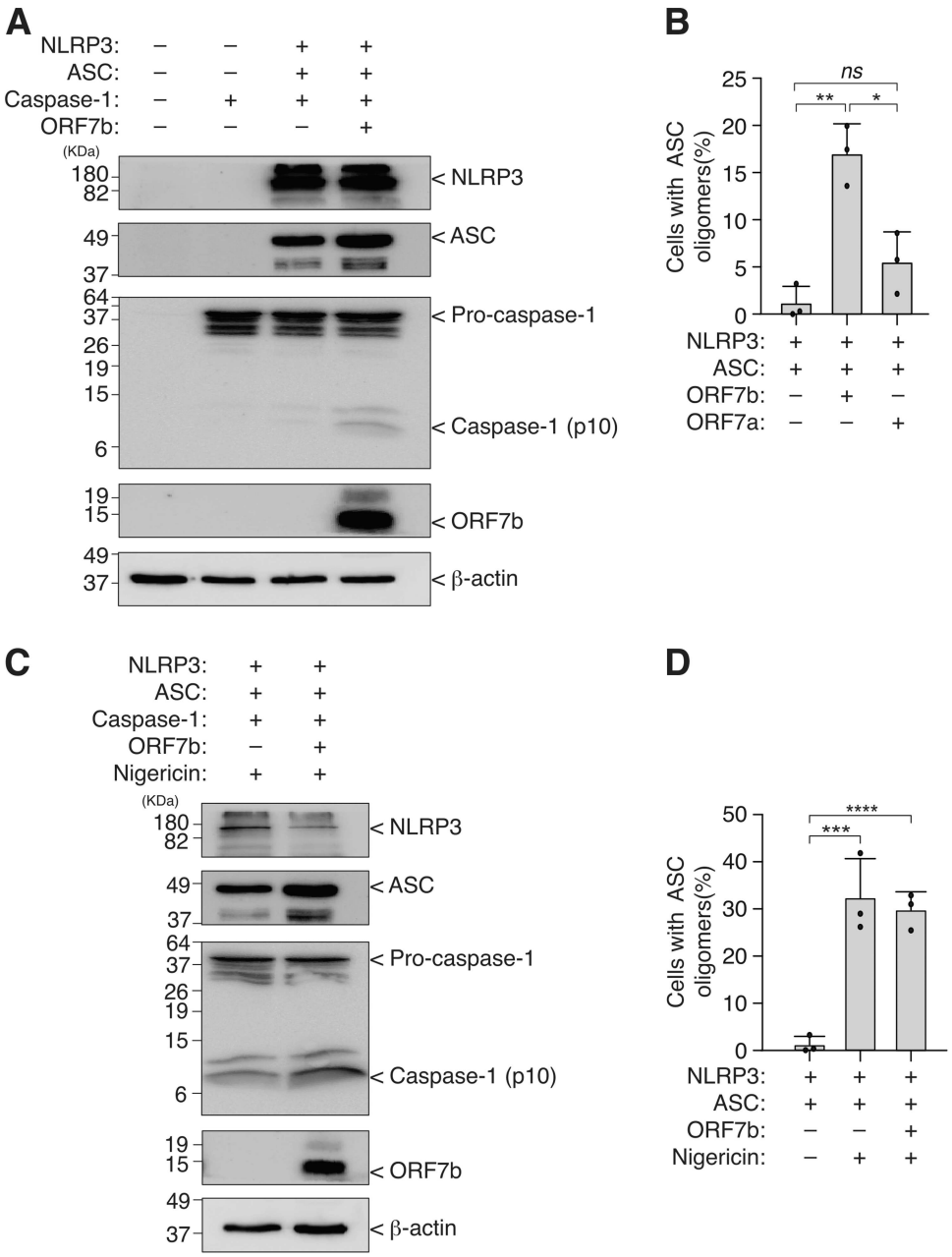

FIGURE 2 | ORF7b from SARS-CoV-2 induces NLRP3 inflammasome activation. (A) Western blot for NLRP3, ASC, caspase-1, ORF7b and β-actin for HEK293T cells after 24 h of transfection with empty pcDNA vector (–) or plasmids encoding for SARS-CoV-2 ORF7b, NLRP3, ASC and caspase-1 as indicated (+). Western blot representative of three independent experiments. (B) Percentage of cells with ASC oligomers determined by flow cytometry. Cells were transfected as in A but with plasmids encoding for SARS-CoV-2 ORF7a or ORF7b proteins as indicated (+). (C) Western blot of cells transfected as in A but treated or not with nigericin (10 μM) for 30 min. Western blot representative of three independent experiments. (D) Percentage of cells with ASC oligomers determined by flow cytometry. Cells were transfected and treated as in C. For B,D each dot represents an independent experiment, and data are represented as mean (grey bars) ± s.e.m. One-way ANOVA with Holm-Sidak's multiple-comparisons test was used for B,D; ****$p < 0.0001$, ***$p > 0.0001 < 0.001$, **$p > 0.001 < 0.01$, *$p > 0.01 < 0.05$, $p > 0.05$ not significant (*ns*).

arise the question if all NLRP3 puncta are active receptor and besides dispersed TGN structures, NLRP3 could also binds to other cellular structures, as it has been shown for mitochondria, endosomes or the microtubule-organizing centre [44–50].

The limitation of our study includes by one hand that mechanistically we have not formally shown that ORF7b TGN dispersion is promoting NLRP3 inflammasome activation. However, there are several previous studies, at mechanistic and structural level, showing that dispersed TGN vesicles promotes interaction with NLRP3 and favours its activation [30, 43, 49, 51–54]. Also, most airway epithelial cells do not express endogenous NLRP3 [22], while myeloid cells, with increase NLRP3 expression, lack the ACE2 receptor for SARS-CoV-2 infection [19]. However, during infection, NLRP3 expression could be increased in infected or activated airway epithelial cells. Therefore, it is necessary to prove NLRP3 activation by ORF7b in a relevant cellular model of SARS-CoV-2 infection.

10969071, 2026, 4, Downloaded from https://onlinelibrary.wiley.com/doi/10.1002/jmv.70894 by Servicio Murciano De Salud, Wiley Online Library on [31/03/2026]. See the Terms and Conditions (https://onlinelibrary.wiley.com/terms-and-conditions) on Wiley Online Library for rules of use; OA articles are governed by the applicable Creative Commons License

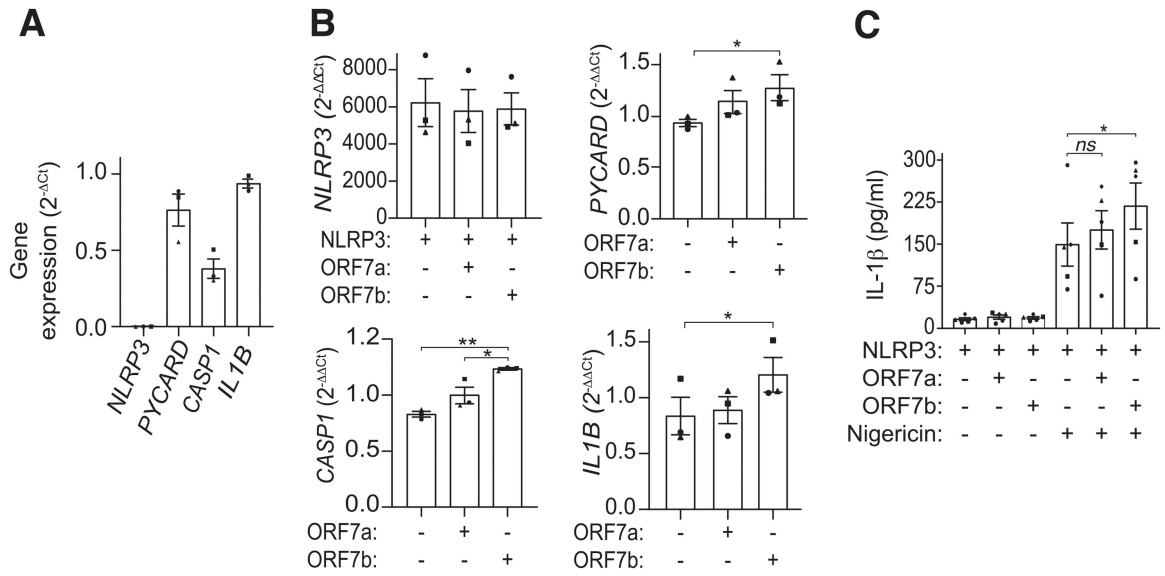

FIGURE 3 | IL-1β release is potentiated in human primary small airway epithelial cells by SARS-CoV-2 ORF7b expression. (A) Expression of inflammasome genes in human primary small airway epithelial cells (HSAEC). (B) Expression of inflammasome genes in HSAEC cells transfected with plasmids encoding for NLRP3 and SARS-CoV-2 ORF7a or ORF7b as indicated. (C) ELISA of IL-1β in HSAEC supernatants transfected for 24 h with NLRP3 and SARS-CoV-2 ORF7a or ORF7b as indicated and then treated or not with nigericin (10 μM) for 24 h. Each symbol represents an independent experiment performed in duplicate biological replicates, and data are represented as mean ± s.e.m; Paired *t*-test was used for B,C; $^{**}p > 0.001 < 0.01$, $^{*}p > 0.01 < 0.05$, $p > 0.05$ not significant (*ns*).

In conclusion, our study shows that the expression of the SARS-CoV-2 protein ORF7b facilitates and increase NLRP3 inflammasome activation, as well as it disperses the TGN, suggesting that SARS-CoV-2 could be modulating host immune system by activating NLRP3 by different activation pathways and contributing to COVID-19 symptoms severity.

4 | Material and Methods

Reagents. Different reagents and their sources used in this assay were: nigericin sodium salt was from Sigma-Aldrich, Lipofectamine 2000 was from Life Technologies. The composition of the E-total (Et) buffer used in all the experiment to stimulate cells with nigericin was as follows: 147 mM NaCl, 10 mM HEPES, 13 mM glucose, 2 mM $CaCl_2$, 1 mM $MgCl_2$, and 2 mM KCl; pH 7.4.

Plasmid constructions. Different constructs of SARS-CoV-2 proteins were from Addgene or from GeneScript and cloned either into the pGBW + C-HA (Gateway Binary Vector) or pcDNA vector: Nsp2 (Accession code YP_009725298.1), Nsp4 (Accession code YP_009725300.1), Nsp5 (Accession code YP_009725301.1), Nsp6 (Accession code YP_009725302.1), Nsp7 (Accession code YP_009725303.1), Nsp8 (Accession code YP_009725304.1, Nsp9 (Accession code YP_009725305.1), Nsp10 (Accession code YP_009725306.1), Nsp11 (Accession code YP_009725312.1), Nsp13 (Accession code YP_009725308.1), Spike protein (S protein, ORF2; GeneID 43740568), Envelope protein (E protein; GeneID 43740570), Membrane protein (M protein; GeneID 43740571) and Nucleocapsid phosphoprotein (N protein, ORF9; GeneID 43740575). Likewise, other constructs for SARS-CoV-2 proteins expression were ordered from GenScript and cloned into pcDNA3.1 + C-HA vector: Nsp1 (Accession code YP_009725297.1), Nsp12 (Accession code YP_009725307.1), Nsp14 (Accession code YP_009725309.1), Nsp15 (Accession code YP_009725310.1), Nsp16 (Accession code YP_009725311.1), Envelope protein (E protein, ORF4; GeneID 43740570), ORF3a (GeneID 43740571) ORF6 (GeneID 43740572), ORF7a (GeneID 43740573), ORF7b (GeneID 43740574), ORF8 (GeneID 43740577) and ORF10 (GeneID 43740576). Human NLRP3 (UniProt Q96P20) tagged with YFP expression vector was from previous studies [32], human pro-caspase1 (UniProt P29466) expression vector was kindly provided by George R. Dubyak Group (Case Western Reserve University, Cleveland, OH, US) and human ASC (Uniprot Q9ULZ3) expression vector tagged with RFP at the C terminus was kindly provided by Eicke Latz (University Hospital Bonn, Germany). Plasmid construct expressing the red fluorescent protein of Discosoma sp. was used as transfection control (pDsRed1-N1, Clontech).

Cells and transfections. HEK293T cells (CRL-11268, American Type Culture Collection) and HEK293T cells stably expressing the human NLRP3-YFP [32] were maintained in Dulbecco's modified Eagle's medium (DMEM)/F-12 (1:1) (Lonza) supplemented with 10% fetal calf serum (FCS) (Life Technologies), 2 mM GlutaMAX (Life Technologies), 1% penicillin-streptomycin (Life Technologies), and for stable cell line media was supplemented with G418 (2 mg/mL; Acros Organics).

Human primary small airway epithelial cells (HSAEC, ATCC PCS-301-010) were cultured in Airway Epithelial Cell Basal Medium (ATCC) complemented with hyaluronic acid supplement (500 mg/mL), linoleic acid (0.6 mM), lecithin (0.6 mg/mL), L-glutamine (6 mM), P extract (0.4%) and with the Bronchial Epithelial Growth Kit containing 1.0 mM epinephrine, 5 mg/mL transferrin, 10 nM T3, 5 mg/mL hydrocortisone, 5 ng/mL recombinant human epithelial growth factor (EGF), and 5 mg/mL recombinant human insulin (ATCC).

All cell cultures were maintained at 37°C in a humidified 5% CO_2 incubator and all cells were routinely tested for

10969071, 2026, 4, Downloaded from https://onlinelibrary.wiley.com/doi/10.1002/jmv.70894 by Servicio Murciano De Salud, Wiley Online Library on [31/03/2026]. See the Terms and Conditions (https://onlinelibrary.wiley.com/terms-and-conditions) on Wiley Online Library for rules of use; OA articles are governed by the applicable Creative Commons License

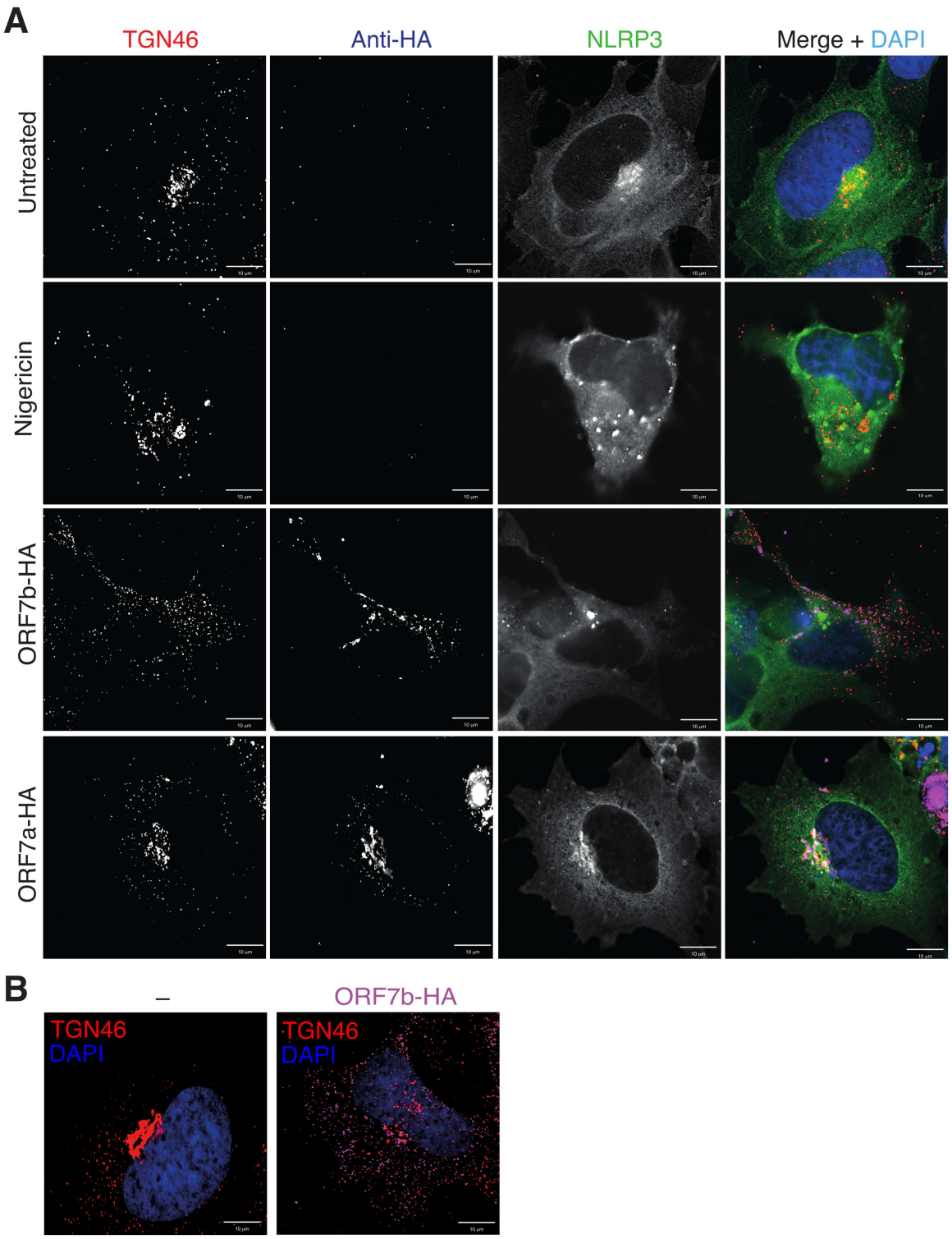

FIGURE 4 | Trans-Golgi network is dispersed by SARS-CoV-2 ORF7b protein. (A) Representative images of HEK293T cells stably expressing NLRP3-YFP (green) and transfected for 48 h with SARS-CoV-2 ORF7a or ORF7b as indicated, treated or not with nigericin (10 μM) for 1.5 h. The trans-Golgi was stained with the TGN46 marker (red), ORF7a or ORF7b was stained with anti-HA antibody (purple) and nuclei was detected with DAPI (blue). Scale bar: 10 μm. Representative images from six independent experiments. (B) Representative images of HEK293T cells transfected for 48 h with SARS-CoV-2 with empty pcDNA vector (left) or ORF7b-HA (right). The trans-Golgi was stained with the TGN46 marker (red), ORF7b was stained with anti-HA antibody (purple) and nuclei was detected with DAPI (blue). Scale bar: 10 μm. Representative images from six independent experiments.

mycoplasma contamination with the Mycoplasma Detection Kit (Roche). Lipofectamine 2000 was used for the transfection of cells according to the manufacturer's instructions using the indicated amount of plasmid.

Quantitative PCR. HSAEC cells were washed twice with phosphate-buffered saline (PBS) before total RNA purification using the RNeasy kit (Qiagen) following the manufacturer's recommendations and RNA was quantified on a NanoDrop

10969071, 2026, 4, Downloaded from https://onlinelibrary.wiley.com/doi/10.1002/jmv.70894 by Servicio Murciano De Salud, Wiley Online Library on [31/03/2026]. See the Terms and Conditions (https://onlinelibrary.wiley.com/terms-and-conditions) on Wiley Online Library for rules of use; OA articles are governed by the applicable Creative Commons License

2000 (Thermo Fisher Scientific). 700 ng of RNA was reverse transcribed using an iScriptTM cDNA synthesis kit (BioRad). qPCR was performed using a CFX96 Touch Real-Time PCR detection System (BioRad) with SYBR Green mix (Takara) and the primers used were obtained from Sigma-Aldrich (KiCqStart Primers) and Quiagen (QuantiTect Primer Assay) (Supporting Table 2). Relative gene expression was calculated using the $2^{-\Delta Ct}$ method or the $2^{-\Delta\Delta Ct}$ method, normalizing gene expression to *HPRT1* expression as an endogenous control.

Flow cytometry. Intracellular ASC-RFP-speck formation was evaluated by Time-of-Flight inflammasome evaluation technique, as previously described [55]. Briefly, HEK293T cells were transiently transfected with ASC-RFP, YFP-NLRP3 and ORF7a or ORF7b SARS-CoV-2. 24 h post-transfection, cells were treated or not with nigericin (10 μM) for 30 min and, subsequently, the detection of ASC-specking cells was analysed by flow cytometry (Supporting Figure 4) using FACS Canto (BD Biosciences) and the FCS express software (De Novo Software).

Western blot. HEK293T cells were lysed on ice-cold lysis buffer (50 mM Tris-HCl pH 8.0, 150 mM NaCl, 2% Triton X-100, supplemented with 100 μL/mL of protease inhibitor mixture from Sigma-Aldrich) for 30 min on ice and were then clarified by centrifugation at 13,052 *xg* for 10 min at 4°C. Cell lysates were mixed with loading buffer (Sigma), boiled at 9°C for 5 min, resolved in 12% to 15% polyacrylamide gels (Bio-Rad) and transferred to nitrocellulose membranes (Bio-Rad). Different primary antibodies were used for the detection of interest proteins: anti-HA Tag rabbit polyclonal antibody (clone SG77, catalogue 71-5500, ThermoFisher; 1:1000), anti-ASC mouse monoclonal antibody (clone O93E9, catalogue 676502, Biolegend; 1:250), anti-NLRP3/NALP3 mouse monoclonal antibody (clone Cryo-2, catalogue AG-20B-0014, AdipoGen; 1:1000) and horseradish peroxidase (HRP) anti-β-Actin (clone C4, catalogue sc-47778HRP, Santa Cruz Biotechnology; 1:10,000). Appropriate secondary antibody conjugated with HRP was used at 1:5000 dilution (Sigma) and developed with ECL plus (Amhershan Biosciences) in a ChemiDoc HDR (BioRad). Uncropped Western blots are shown in Supporting Figure 5.

Fluorescence microscopy. HEK293T expressing NLRP3-YFP were transfected in poly-L-lysine–coated coverslips (Corning). Cells were washed twice with PBS, fixed for 15 min at room temperature with 4% paraformaldehyde (Electron Microscopy Sciences), and then washed three times with PBS. Cells were then blocked with 2% bovine serum albumin and permeabilized with 0.1% Triton X-100 (Sigma-Aldrich) for 40 min at room temperature. Cells were stained overnight at 4°C with different primary antibodies: anti-HA Tag rabbit polyclonal antibody (clone SG77, catalogue 71-5500, Thermo Fisher; 1:10,000), sheep anti-TGN46 polyclonal antibody (catalogue AHP500GT, Bio-Rad, 1:10,000). Cells were washed and then incubated for 1 h at room temperature with anti-sheep immunoglobulin G (IgG) fluorescence-conjugated secondary antibody (Alexa 647 donkey anti-sheep IgG (H + L), Abcam; 1:2000) or with anti-rabbit immunoglobulin G (IgG) fluorescence-conjugated secondary antibody (Alexa 555 donkey anti-rabbit IgG (H + L), Life Technologies; 1:2000). Cells were washed and nuclei were stained for 10 min with 4′,6-diamidino-2-phenylindole (DAPI, 1:10,000; Sigma-Aldrich), and coverslips were mounted on slides with mounting medium (S3023, Dako).

To analyse NLRP3-YFP puncta distribution cells were co-transfected with the different SARS-CoV-2 plasmid constructions and pDsRed1-N1. In some experiments, cells were treated with nigericin (10 μM), MCC950 (10 μM) or with a buffer containing 40 μM KCl. MCC950 inhibitor was applied 1 h after of the transfection of SARS-CoV-2 constructs. 48 h after transfection cells expressing DsRed with or without NLRP3 puncta distribution were counted from nine different fields in each coverslip. The percentage of cells with NLRP3 puncta distribution was then calculated over the total number of DsRed positive cells.

Images were acquired using a Nikon Eclipse Ti microscope equipped with a 20x S Plan Fluor objective (numerical aperture 0.45), a 60x Plan Apo Vc objective (numerical aperture 1.40), and a digital Sight DS-QiMc camera (Nikon), 387-/447-nm, 472-/520-nm, 543-/593-nm, and 650-/668-nm filter sets (Semrock) and the NIS-Elements AR software (Nikon). Images were analysed with ImageJ (U.S. National Institutes of Health) and deconvolution was performed with the Parallel Iterative Deconvolution plugin for iterative image deblurring [56].

ELISA assay. Human IL-1β was detected in cell supernatants using the IL-1 beta Human Instant ELISA™ Kit from Invitrogen following the manufacturer's instructions and then readed in a Synergy Mx (BioTek) plate reader.

Viral ORF7b sequence analysis. The different ORF7b viral sequences were obtained from the National Center for Biotechnology Information server (www.ncbi.nlm.nih.gov/labs/virus/vssi/#), and the existing variants were chosen according to the Nextstrain naming system for variants (www.covariants.org/variants). Multiple sequence alignment was performed with the CLUSTALW program of the European Bioinformatics Institute (www.ebi.ac.uk/Tools/msa/clustalo).

Statistical and data analysis. Statistical analyses were performed using GraphPad Prism v.9 (GraphPad Software Inc). Normality and distribution of the samples was determined with Shapiro-Wilk normality test. Comparisons of multiple groups with normal distribution were analysed by one-way analysis of variance ANOVA with Holm-Sidak's multiple-comparisons test. For groups not following normality, the Kruskal-Wallis test was used to compare multiple groups. Two paired groups with normal distribution were analysed by the paired *t*-test. All data are shown as mean values and errors bars represent standard error (s.e.m.), *p* value is indicated as $^{****}p < 0.0001$; $^{***}p > 0.0001 < 0.001$; $^{**}p > 0.001 < 0.01$; $^{*}p > 0.01 < 0.05$; $p > 0.05$ not significant (*ns*).

Author Contributions

Julio García-Villalba, Laura Hurtado-Navarro, Diego Angosto-Bazarra, experimental execution. Julio García-Villalba, Laura Hurtado-Navarro, Diego Angosto-Bazarra, Alberto Baroja-Mazo, Pablo Pelegrin, data analysis. Alberto Baroja-Mazo, Diego Angosto-Bazarra and Pablo Pelegrin conceived the experiments. Julio García-Villalba, Laura Hurtado-Navarro and Pablo Pelegrin prepared the figures and wrote the paper. Pablo Pelegrin provided funding and overall supervision of the study.

Acknowledgments

We thank George R. Dubyak (Case Western Reserve University, Cleveland, OH, US) and Eicke Latz (University Hospital Bonn,

10969071, 2026, 4, Downloaded from https://onlinelibrary.wiley.com/doi/10.1002/jmv.70894 by Servicio Murciano De Salud, Wiley Online Library on [31/03/2026]. See the Terms and Conditions (https://onlinelibrary.wiley.com/terms-and-conditions) on Wiley Online Library for rules of use; OA articles are governed by the applicable Creative Commons License

Germany) for expression vectors, A.I. Gomez (IMIB, Murcia, Spain) for technical assistance with molecular and cellular biology, and the members of the Pelegrin's laboratory for comments and suggestions throughout the development of this project. This work was supported by grants to P.P. from MCIN/AEI/10.13039/501100011033 (grants PID2020-116709RB-I00, PID2023-147531OB-I00, CNS2022-135105 and RED2022-134511-T), Fundación Séneca (grants 0003/COVI/20, 21897/PI/22 and 23028/GERM/25), the Instituto Salud Carlos III (grant AC22/00009). J.G-V. was supported by the fellowship IFI22/00031 (Instituto Salud Carlos III) and L.H-N. was supported by the fellowship 21214/FPI/19 (*Fundación Séneca, Región de Murcia*, Spain).

Conflicts of Interest

LH-N, DA-B, AB-M, and PP are co-founders of Viva in vitro diagnostics SL. PP is inventor in patent application PCT/EP2020/056729. The other authors have no conflict of interest declared.

Data Availability Statement

The data that support the findings of this study are available from the corresponding author upon reasonable request.

References

1. P. Broz, P. Pelegrín, and F. Shao, "The Gasdermins, a Protein Family Executing Cell Death and Inflammation," *Nature Reviews Immunology* 20, no. 3 (2020): 143–157, https://doi.org/10.1038/s41577-019-0228-2.

2. K. V. Swanson, M. Deng, and J. P. Y. Ting, "The NLRP3 Inflammasome: Molecular Activation and Regulation to Therapeutics," *Nature Reviews Immunology* 19, no. 8 (2019): 477–489, https://doi.org/10.1038/s41577-019-0165-0.

3. D. Angosto-Bazarra, C. Alarcón-Vila, L. Hurtado-Navarro, M. C. Baños, J. Rivers-Auty, and P. Pelegrín, "Evolutionary Analyses of the Gasdermin Family Suggest Conserved Roles in Infection Response Despite Loss of Pore-Forming Functionality," *BMC Biology* 20, no. 1 (2022): 9, https://doi.org/10.1186/s12915-021-01220-z.

4. B. V. Tsu, R. Agarwal, N. S. Gokhale, et al., "Host-Specific Sensing of Coronaviruses and Picornaviruses by the CARD8 Inflammasome," *PLoS Biology* 21, no. 6 (2023): e3002144, https://doi.org/10.1371/journal.pbio.3002144.

5. P. Pan, M. Shen, Z. Yu, et al., "SARS-CoV-2 N Protein Promotes NLRP3 Inflammasome Activation to Induce Hyperinflammation," *Nature Communications* 12, no. 1 (2021): 4664, https://doi.org/10.1038/s41467-021-25015-6.

6. M. H. Liu, X. L. Lin, and L. L. Xiao, "SARS-CoV-2 Nucleocapsid Protein Promotes TMAO-Induced NLRP3 Inflammasome Activation by SCAP–SREBP Signaling Pathway," *Tissue and Cell* 86 (2024): 102276, https://doi.org/10.1016/j.tice.2023.102276.

7. X. Huang, W. Zhu, H. Zhang, S. Qiu, and H. Shao, "SARS-CoV-2 N Protein Induces Alveolar Epithelial Apoptosis via NLRP3 Pathway in ARDS," *International Immunopharmacology* 144 (2025): 113503, https://doi.org/10.1016/j.intimp.2024.113503.

8. S. Yang, M. Li, G. Lian, Y. Wu, J. Cui, and L. Wang, "ABHD8 Antagonizes Inflammation by Facilitating Chaperone-Mediated Autophagy-Mediated Degradation of NLRP3," *Autophagy* 21, no. 2 (2025): 338–351, https://doi.org/10.1080/15548627.2024.2395158.

9. S. J. Theobald, A. Simonis, T. Georgomanolis, et al., "Long-Lived Macrophage Reprogramming Drives Spike Protein-Mediated Inflammasome Activation in COVID-19," *EMBO Molecular Medicine* 13 (2021): 1–20.

10. M. Z. Ratajczak, K. Bujko, A. Ciechanowicz, et al., "SARS-CoV-2 Entry Receptor ACE2 Is Expressed on Very Small CD45- Precursors of Hematopoietic and Endothelial Cells and in Response to Virus Spike Protein Activates the Nlrp3 Inflammasome," *Stem Cell Reviews and Reports* 17, no. 1 (2021): 266–277, https://doi.org/10.1007/s12015-020-10010-z.

11. E. A. Albornoz, A. A. Amarilla, N. Modhiran, et al., "SARS-CoV-2 Drives NLRP3 Inflammasome Activation in Human Microglia Through Spike Protein," *Molecular Psychiatry* 28, no. 7 (2023): 2878–2893, https://doi.org/10.1038/s41380-022-01831-0.

12. M. Yalcinkaya, W. Liu, M. N. Islam, et al., "Modulation of the NLRP3 Inflammasome by Sars-CoV-2 Envelope Protein," *Scientific Reports* 11, no. 1 (2021): 24432, https://doi.org/10.1038/s41598-021-04133-7.

13. J. W. Guarnieri, A. Angelin, D. G. Murdock, et al., "SARS-COV-2 Viroporins Activate the NLRP3-Inflammasome by the Mitochondrial Permeability Transition Pore," *Frontiers in Immunology* 14 (2023): 1064293, https://doi.org/10.3389/fimmu.2023.1064293.

14. H. Xu, I. A. Akinyemi, S. A. Chitre, et al., "SARS-CoV-2 Viroporin Encoded by ORF3a Triggers the NLRP3 Inflammatory Pathway," *Virology* 568, no. January (2022): 13–22, https://doi.org/10.1016/j.virol.2022.01.003.

15. I. Y. Chen, M. Moriyama, M. F. Chang, and T. Ichinohe, "Severe Acute Respiratory Syndrome Coronavirus Viroporin 3a Activates the NLRP3 Inflammasome," *Frontiers in Microbiology* 10 (2019): 50, https://doi.org/10.3389/fmicb.2019.00050.

16. X. Wu, M. K. Manske, G. J. Ruan, et al., "Secreted ORF8 Induces Monocytic Pro-Inflammatory Cytokines Through NLRP3 Pathways in Patients With Severe COVID-19," *iScience* 26, no. 6 (2023): 106929, https://doi.org/10.1016/j.isci.2023.106929.

17. C. S. Shi, N. R. Nabar, N. N. Huang, and J. H. Kehrl, "SARS-Coronavirus Open Reading Frame-8b Triggers Intracellular Stress Pathways and Activates NLRP3 Inflammasomes," *Cell Death Discovery* 5, no. 1 (2019): 101, https://doi.org/10.1038/s41420-019-0181-7.

18. E. Zodda, M. Pons, N. DeMoya-Valenzuela, et al., "Induction of the Inflammasome by the SARS-CoV-2 Accessory Protein ORF9b, Abrogated by Small-Molecule ORF9b Homodimerization Inhibitors," *Journal of Medical Virology* 97, no. 2 (2025): e70145, https://doi.org/10.1002/jmv.70145.

19. L. I. Labzin, K. Y. Chew, K. Eschke, et al., "Macrophage ACE2 is Necessary for SARS-CoV-2 Replication and Subsequent Cytokine Responses That Restrict Continued Virion Release," *Science Signaling* 16, no. 782 (2023): eabq1366, https://doi.org/10.1126/scisignal.abq1366.

20. C. Junqueira, Â. Crespo, S. Ranjbar, et al., "FcγR-Mediated SARS-CoV-2 Infection of Monocytes Activates Inflammation," *Nature* 606 (2022): 576–584, https://doi.org/10.1038/s41586-022-04702-4.

21. E. Sefik, R. Qu, C. Junqueira, et al., "Inflammasome Activation in Infected Macrophages Drives COVID-19 Pathology," *Nature* 606 (2022): 585–593, https://doi.org/10.1038/s41586-022-04802-1.

22. R. Planès, M. Pinilla, K. Santoni, et al., "Human NLRP1 is a Sensor of Pathogenic Coronavirus 3CL Proteases in Lung Epithelial Cells," *Molecular Cell* 82, no. 13 (2022): 2385–2400.e9, https://doi.org/10.1016/j.molcel.2022.04.033.

23. S. Amin, S. Aktar, M. M. Rahman, and M. M. Hassan Chowdhury, "NLRP3 Inflammasome Activation in COVID-19: An Interlink Between Risk Factors and Disease Severity," *Microbes and Infection* 110, no. 2 (2021): 104913.

24. J. Courjon, O. Dufies, A. Robert, et al., "Heterogeneous NLRP3 Inflammasome Signature in Circulating Myeloid Cells as a Biomarker of COVID-19 Severity," *Blood Advances* 5, no. 5 (2021): 1523–1534, https://doi.org/10.1182/bloodadvances.2020003918.

25. T. S. Rodrigues, K. S. G. de Sá, A. Y. Ishimoto, et al., "Inflammasomes Are Activated in Response to SARS-CoV-2 Infection and Are Associated With COVID-19 Severity in Patients," *Journal of Experimental Medicine* 218, no. 3 (2021): e20201707, https://doi.org/10.1084/jem.20201707.

26. Q. Zhang, P. Bastard, C. O. V. I. D. Human Genetic Effort, A. Cobat, and J. L. Casanova, "Human Genetic and Immunological Determinants of Critical COVID-19 Pneumonia," *Nature* 603 (2022): 587–598.

10969071, 2026, 4, Downloaded from https://onlinelibrary.wiley.com/doi/10.1002/jmv.70894 by Servicio Murciano De Salud, Wiley Online Library on [31/03/2026]. See the Terms and Conditions (https://onlinelibrary.wiley.com/terms-and-conditions) on Wiley Online Library for rules of use; OA articles are governed by the applicable Creative Commons License

27. Y. R. Guo, Q. D. Cao, Z. S. Hong, et al., "The Origin, Transmission and Clinical Therapies on Coronavirus Disease 2019 (COVID-19) Outbreak—An Update on the Status," *Military Medical Research* 7, no. 1 (2020): 11, https://doi.org/10.1186/s40779-020-00240-0.

28. M. S. Abers, O. M. Delmonte, E. E. Ricotta, et al., "An Immune-Based Biomarker Signature Is Associated With Mortality in COVID-19 Patients," *JCI Insight* 6, no. 1 (2021): 144455, https://doi.org/10.1172/jci.insight.144455.

29. E. Kyriazopoulou, P. Panagopoulos, S. Metallidis, et al., "An Open Label Trial of Anakinra to Prevent Respiratory Failure in COVID-19," *eLife* 10, no. Il (2021): 1–21, https://doi.org/10.7554/eLife.66125.

30. J. Chen and Z. J. Chen, "PtdIns4P on Dispersed Trans-Golgi Network Mediates NLRP3 Inflammasome Activation," *Nature* 564, no. 7734 (2018): 71–76, https://doi.org/10.1038/s41586-018-0761-3.

31. B. S. Saller, S. Wöhrle, L. Fischer, et al., "Acute Suppression of Mitochondrial ATP Production Prevents Apoptosis and Provides an Essential Signal for NLRP3 Inflammasome Activation," *Immunity* 58, no. 1 (2025): 90–107.e11, https://doi.org/10.1016/j.immuni.2024.10.012.

32. A. Tapia-Abellán, D. Angosto-Bazarra, C. Alarcón-Vila, et al., "Sensing Low Intracellular Potassium by NLRP3 Results in a Stable Open Structure That Promotes Inflammasome Activation," *Science Advances* 7, no. 38 (2021): eabf4468, https://doi.org/10.1126/sciadv.abf4468.

33. Y. Duan, L. Zhang, D. Angosto-Bazarra, P. Pelegrín, G. Núñez, and Y. He, "RACK1 Mediates NLRP3 Inflammasome Activation by Promoting NLRP3 Active Conformation and Inflammasome Assembly," *Cell Reports* 33, no. 7 (2020): 108405, https://doi.org/10.1016/j.celrep.2020.108405.

34. P. M. Soriano-Teruel, G. García-Laínez, M. Marco-Salvador, et al., "Identification of an ASC Oligomerization Inhibitor for the Treatment of Inflammatory Diseases," *Cell Death & Disease* 12, no. 12 (2021): 1155, https://doi.org/10.1038/s41419-021-04420-1.

35. R. C. Coll, K. Schroder, and P. Pelegrín, "NLRP3 and Pyroptosis Blockers for Treating Inflammatory Diseases," *Trends In Pharmacological Sciences* 43, no. 8 (2022): 653–668, https://doi.org/10.1016/j.tips.2022.04.003.

36. J. Zeng, X. Xie, X. L. Feng, et al., "Specific Inhibition of the NLRP3 Inflammasome Suppresses Immune Overactivation and Alleviates COVID-19 Like Pathology in Mice," *EBioMedicine* 75 (2022): 103803, https://doi.org/10.1016/j.ebiom.2021.103803.

37. X. Wu, M. K. Manske, G. Ruan, K. E. Nowakowski, and P. Jithma, "Secreted ORF8 is a Pathogenic Cause of Severe Covid-19 and Potentially Targetable With Select NLRP3 Inhibitors," *bioRxiv* 1 (2021): 470978, https://doi.org/10.1101/2021.12.02.470978.

38. N. E. Kim, D. K. Kim, and Y. J. Song, "SARS-CoV-2 Nonstructural Proteins 1 and 13 Suppress Caspase-1 and the NLRP3 Inflammasome Activation," *Microorganisms* 9, no. 3 (2021): 494, https://doi.org/10.3390/microorganisms9030494.

39. J. Ma, F. Zhu, M. Zhao, et al., "SARS-CoV-2 Nucleocapsid Suppresses Host Pyroptosis by Blocking Gasdermin D Cleavage," *EMBO Journal* 40, no. 18 (2021): 1–17, https://doi.org/10.15252/embj.2021108249.

40. B. Malone, N. Urakova, E. J. Snijder, and E. A. Campbell, "Structures and Functions of Coronavirus Replication–Transcription Complexes and Their Relevance for SARS-CoV-2 Drug Design," *Nature Reviews Molecular Cell Biology* 23, no. 1 (2022): 21–39, https://doi.org/10.1038/s41580-021-00432-z.

41. S. R. Schaecher, M. S. Diamond, and A. Pekosz, "The Transmembrane Domain of the Severe Acute Respiratory Syndrome Coronavirus ORF7b Protein is Necessary and Sufficient for Its Retention in the Golgi Complex," *Journal of Virology* 82, no. 19 (2008): 9477–9491, https://doi.org/10.1128/JVI.00784-08.

42. N. Redondo, S. Zaldívar-López, J. J. Garrido, and M. Montoya, "SARS-CoV-2 Accessory Proteins in Viral Pathogenesis: Knowns and Unknowns," *Frontiers in Immunology* 12 (2021): 708264, https://doi.org/10.3389/fimmu.2021.708264.

43. K. P. Pandey and Y. Zhou, "Influenza A Virus Infection Activates NLRP3 Inflammasome Through Trans-Golgi Network Dispersion," *Viruses* 14, no. 1 (2022): 88, https://doi.org/10.3390/v14010088.

44. M. Pizzuto and P. Pelegrin, "Cardiolipin in Immune Signaling and Cell Death," *Trends in Cell Biology* 30, no. 11 (2020): 892–903, https://doi.org/10.1016/j.tcb.2020.09.004.

45. E. I. Elliott, A. N. Miller, B. Banoth, et al., "Cutting Edge: Mitochondrial Assembly of the NLRP3 Inflammasome Complex Is Initiated at Priming," *Journal of Immunology* 200, no. 9 (2018): 3047–3052, https://doi.org/10.4049/jimmunol.1701723.

46. S. S. Iyer, Q. He, J. R. Janczy, et al., "Mitochondrial Cardiolipin is Required for Nlrp3 Inflammasome Activation," *Immunity* 39, no. 2 (2013): 311–323, https://doi.org/10.1016/j.immuni.2013.08.001.

47. B. Lee, C. Hoyle, R. Wellens, et al., "Disruptions in Endocytic Traffic Contribute to the Activation of the NLRP3 Inflammasome," *Science Signaling* 16, no. 773 (2023): eabm7134, https://doi.org/10.1126/scisignal.abm7134.

48. Z. Zhang, R. Venditti, L. Ran, et al., "Distinct Changes in Endosomal Composition Promote NLRP3 Inflammasome Activation," *Nature Immunology* 24 (2022): 30–41.

49. L. Nie, C. Fei, Y. Fan, et al., "Consecutive Palmitoylation and Phosphorylation Orchestrates NLRP3 Membrane Trafficking and Inflammasome Activation," *Molecular Cell* 84, no. 17 (2024): 3336–3353.e7, https://doi.org/10.1016/j.molcel.2024.08.001.

50. V. G. Magupalli, R. Negro, Y. Tian, et al., "HDAC6 Mediates an Aggresome-Like Mechanism for NLRP3 and Pyrin Inflammasome Activation," *Science* 369, no. 6510 (2020): eaas8995, https://doi.org/10.1126/science.aas8995.

51. L. Andreeva, L. David, S. Rawson, et al., "NLRP3 Cages Revealed by Full-Length Mouse NLRP3 Structure Control Pathway Activation," *Cell* 184, no. 26 (2021): 6299–6312.e22, https://doi.org/10.1016/j.cell.2021.11.011.

52. N. A. Schmacke, F. O'duill, M. M. Gaidt, et al., "IKKβ Primes Inflammasome Formation by Recruiting NLRP3 to the Trans-Golgi Network," *Immunity* 55 (2022): 2271–2284, https://doi.org/10.1016/j.immuni.2022.10.021.

53. D. M. Williams and A. A. Peden, "S-Acylation of NLRP3 Provides a Nigericin Sensitive Gating Mechanism That Controls Access to the Golgi," *eLife* 13 (2024): RP94302, https://doi.org/10.7554/eLife.94302.

54. N. Xiao, A. Kogishi, L. Radochonski, Y. Lei, and J. Chen, "Type A Cholesterol-Dependent Cytolysins Translocate to the Trans-Golgi Network for NLRP3 Inflammasome Activation," *Nature Immunology* 26 (2025): 1673–1685.

55. D. P. Sester, S. J. Thygesen, V. Sagulenko, et al., "A Novel Flow Cytometric Method To Assess Inflammasome Formation," *Journal of Immunology* 194, no. 1 (2014): 455–462, https://doi.org/10.4049/jimmunol.1401110.

56. P. C. Hansen, J. G. Nagy, and D. P. O'Leary, *Deblurring Images: Matrices, Spectra, and Filtering* (Society for Industrial and Applied Mathematics, 2006), https://doi.org/10.1137/1.9780898718874.

Supporting Information

Additional supporting information can be found online in the Supporting Information section.
Supplementary Figure 1: Expression of SARS-CoV-2 proteins. **Supplementary Figure 2:** NLRP3 puncta distribution with the different SARS-CoV- 2 protein expression. **Supplementary Figure 3:** SARS-CoV-2 ORF7b sequence analysis. **Supplementary Figure 4:** Flow cytometry gating strategy. **Supplementary Figure 5:** Uncropped Western blots of Figure 2A,C. **Supplementary Table 1:** Studies reporting inflammasome activation by SARS-CoV- 2. **Supplementary Table 2:** Sequences of the oligonucleotides used in this study.

10969071, 2026, 4, Downloaded from https://onlinelibrary.wiley.com/doi/10.1002/jmv.70894 by Servicio Murciano De Salud, Wiley Online Library on [31/03/2026]. See the Terms and Conditions (https://onlinelibrary.wiley.com/terms-and-conditions) on Wiley Online Library for rules of use; OA articles are governed by the applicable Creative Commons License